

Static recrystallization behavior of hot-deformed magnesium alloy AZ31 during isothermal annealing

YANG Xu-yue(杨续跃)¹, ZHU Ya-kun(朱亚坤)¹, H. MIURA², T. SAKAI²

1. School of Materials Science and Engineering, Central South University, Changsha 410083, China;
2. Department of Mechanical Engineering and Intelligent Systems, University of Electro Communications, Tokyo 182-8585, Japan

Received 23 September 2009; accepted 30 January 2010

Abstract: The static recrystallization of hot-deformed magnesium alloy AZ31 during isothermal annealing was studied at temperature of 503 K by optical and SEM/EBSD metallographic observation. The grain size change during isothermal annealing is categorized into three regions, i.e. an incubation period for grain growth, rapid grain coarsening, and normal grain growth. The number of fine grains per unit area, however, decreases remarkably even in incubation period. This leads to grain coarsening taking place continuously in the whole period of annealing. In contrast, the deformation texture scarcely changes even after full annealing at high temperatures. It is concluded that the annealing processes operating in hot-deformed magnesium alloy with continuous dynamic recrystallized grain structures can be mainly controlled by grain coarsening without texture change, that is, continuous static recrystallization.

Key words: magnesium alloy; AZ31; annealing; continuous recrystallization; grain growth; texture

1 Introduction

Recently, several methods have been adopted for grain refining in Mg alloys with even submicron or nano-crystalline grain size, such as hot and warm rolling[1], hot extrusion at high reduction ratio[2–4], and severe plastic deformation process like equal channel angular extrusion (ECAE)[5–7] and multi-directional forging (MDF)[8]. XING et al[8] studied thermo-mechanical processes for development of ultra-fine grained Mg alloys. They developed fine-grained structures with the grain size of submicrons by using MDF under decreasing temperature conditions and succeeded in much improvement of the plastic workability and also the mechanical properties due to grain refinement.

However, during hot plastic deformation, Mg alloys are liable to undergo rotations of crystal orientation and form strong deformation texture, which further affects the mechanical properties and secondary manufacturing processes[9]. Hence, it is of great importance to reveal the texture forming mechanisms during hot working with concurrent recrystallization[10–12]. Further improve-

ment of the ductility of deformed Mg alloys will be carried through the texture control due to annealing treatment following plastic deformation. There have been few reports on the annealing behaviors of hot-deformed Mg alloys. The knowledge of annealing characteristics and the texture changes in a widely used Mg alloy, e.g. AZ31, appears not aware of existence.

Therefore, the present work aims to investigate the annealing characteristic of Mg alloy AZ31 after hot deformation with strain of 1.2. The microstructural changes taking place during isothermal annealing were systematically studied at 503 K. Changes in the grain structure and, the textures developed during and after hot deformation were analyzed in detail, and the mechanisms of annealing processes were discussed.

2 Experimental

A commercially produced AZ31 Mg alloy was provided as a hot-extruded rod with a diameter of 19 mm. The chemical compositions were as follows: Al 2.68, Zn 0.75, Mn 0.68, Cu 0.001, Si 0.003, Fe 0.003, and balance Mg (mass fraction, %). Cylindrical samples of 8 mm in diameter and 12 mm in height were machined from the

rod parallel to the extrusion direction. Then six evenly spaced annular grooves of 0.12 mm in depth were machined into the end faces of cylinders in order to promote the retention of a graphite lubricant (DAG 154). The samples were annealed at 733 K for 7.2 ks and then furnace cooled, leading to the evolution of equiaxed grains with an average size of about 22 μm .

Compression tests were carried out at constant true strain rates on a testing machine equipped with a water quenching apparatus, which made it possible to quench the samples within 1.5 s after deformation was finished. The samples were deformed up to strain of 1.2 at 573 K at two true strain rates of $3 \times 10^{-3} \text{ s}^{-1}$ and $3 \times 10^{-1} \text{ s}^{-1}$, followed by quenching in water. They were cut to plates with 2–3 mm in thickness parallel to the compression axis, and then isothermally annealed for 10^2 – 10^5 s in air using a muffle furnace at temperatures of 493, 503 and 513 K, respectively. Each plate was mechanically and electrolytically polished and then etched in a mixed solution of 6% picric acid and 94% methanol. The as-deformed and the subsequent annealed microstructures were examined by using optical microscopy (OM) and orientation imaging microscopy (OIM). The distributions of grain size were analyzed by image analysis software of “AnalySIS” (Soft Imaging System Co.). Crystallographical orientation and texture

changes were examined by SEM/OIM.

3 Results and discussion

3.1 Structural changes during annealing

Fig.1 shows a series of typical optical microstructures evolved before and after annealing at 503 K for the hot deformed AZ31 alloy. New grains are not fully developed throughout the material even in high strain, as can be seen in Fig.1(a) and discussed in elsewhere[9]. Figs.1(b)–(d) show that such strain induced new grains coarsen homogeneously with increasing annealing times. After annealing for 10^3 s and below, some rather coarse grains still remain and are clearly distinguishable from surrounding fine grains (Figs.1(b) and (c)), which can be termed as mixed grains states. For annealing time of 10^4 s and above (Fig.1(d)), it is difficult to distinguish the coarse grains from the surrounding ones which coarsen homogeneously, finally leading to a full development of an almost equiaxed grain structure.

Typical grain size distributions of the samples before and after annealing with increasing time are shown in Fig.2. The distribution for annealing time of 10^2 s (Fig.2(b)) is almost similar to that for as-deformed state and shows a bimodal shape with two peaks at

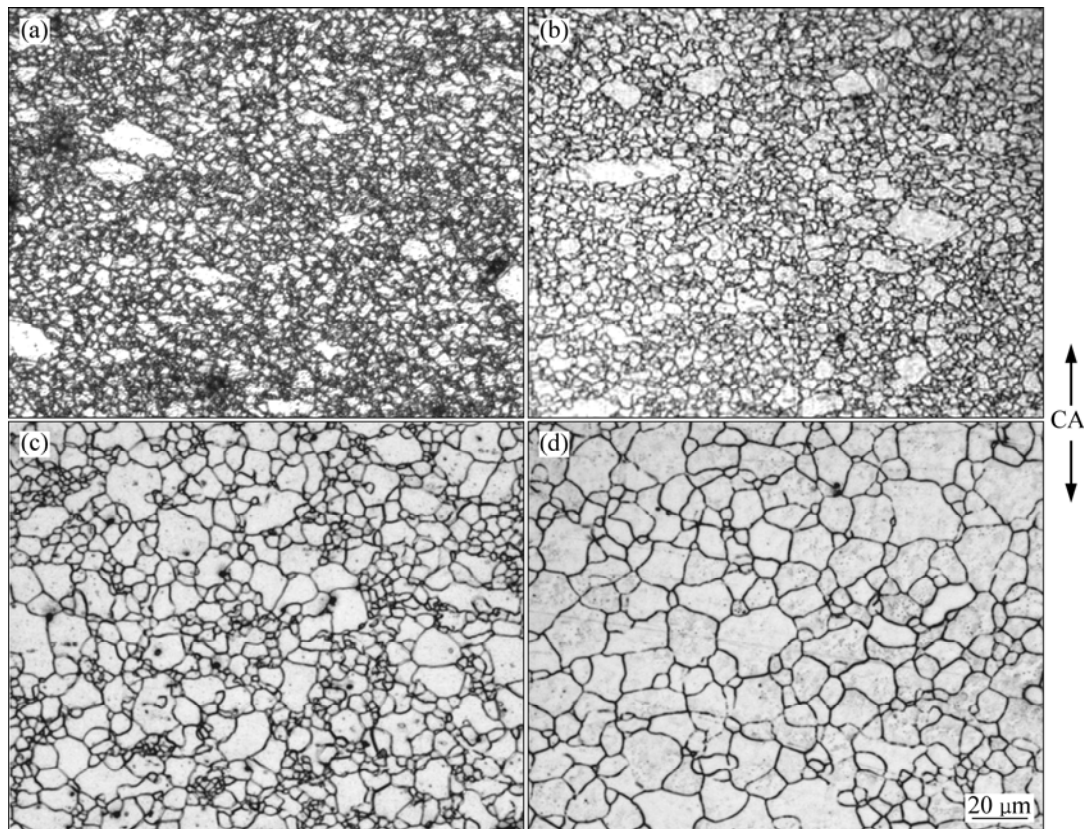


Fig.1 Microstructures evolution in AZ31 alloy deformed to $\varepsilon=1.2$ at 573 K with strain rate of $3 \times 10^{-1} \text{ s}^{-1}$ (a), followed by annealing at 503 K for 10^2 s (b), 10^3 s (c), and 10^4 s (d) (CA indicates compression axis)

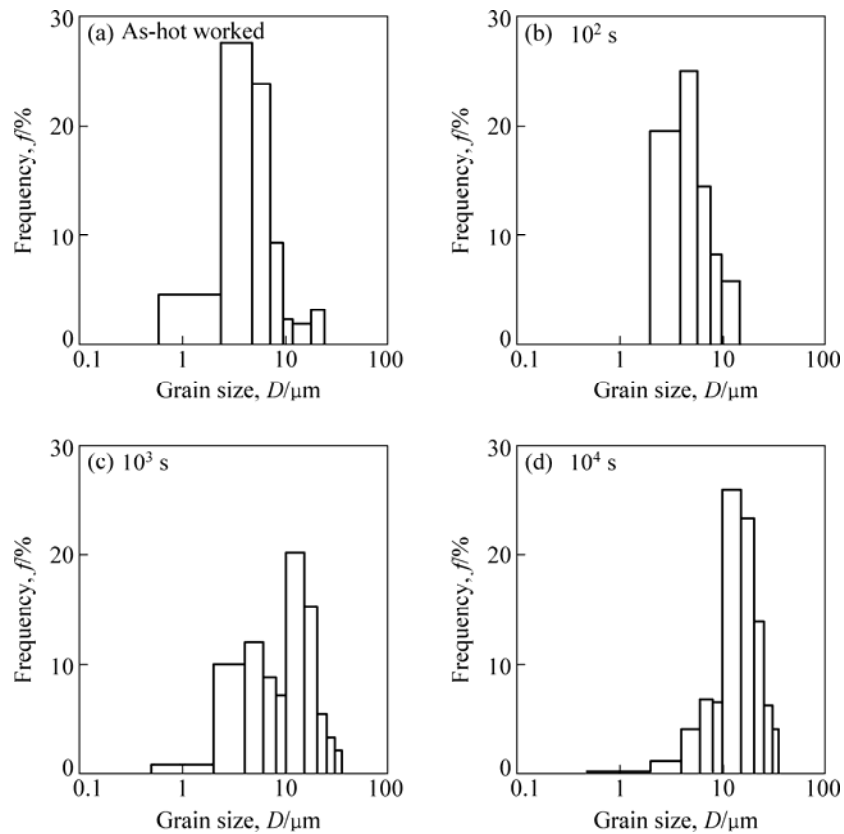


Fig.2 Grain size distribution of sample as function of annealing time at 503 K

around 2 μm and 20 μm. The fine grains correspond to those newly developed grains by hot deformation and the coarser ones correspond to the remained original grains (Fig.2(a)). Upon annealing time over than 10³ s, the fraction of fine grains with ~2 μm rapidly drops with increasing annealing time, leading to changing to a single peak type at around 20 μm (Fig.2(d)).

Fig.3 shows the changes of the average grain size (*D*) in the whole area with annealing temperatures. *D* is hardly changed during annealing time less than 7×10² s, upwards rapidly for 7×10²–7×10⁴ s and then increases slowly with increasing time. Such a grain size change looks like that occurring in conventional cubic metals during annealing[13], and can be categorized into three stages. The time that ranges from 0 to 7×10² s may correspond to an incubation stage for recrystallization, that from 7×10² to 7×10⁴ s to a rapid grain coarsening stage and the longer annealing time above around 7×10⁴ s to a stage for normal grain growth, respectively.

With the increase of annealing temperature from 493 to 513 K, the time at which rapid coarsening begins as well as the time to reach the plateau grain size is reduced (Fig.3). This result is also similar to that of annealing of deformed cubic metals[13]. But the plateau grain size finally reached almost remains constant as annealing temperature rises, differing from that of deformed conventional cubic metals.

Fig.4 shows the changes in the number of fine

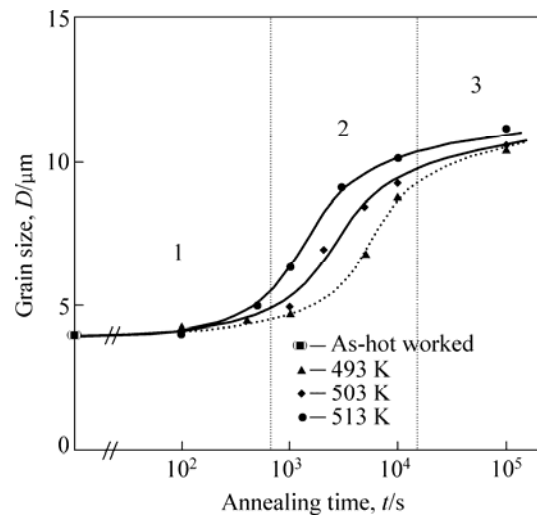


Fig.3 Effect of annealing temperature on average grain size in whole area with time

grains per unit area, *N*, less than 10 μm in diameter with annealing time. It is remarkable to note that *N* drops clearly even in the initial stage of annealing. This is in contrast with the result of the average grain size in Fig.3, i.e. there is no remarkable grain coarsening in this stage. It is concluded from Fig.4 that grain growth starts to take place mainly in the fine-grained regions simultaneously just after annealing even in initial stage (see Figs.2(a)

and 2(b)). Further annealing from 7×10^2 s to 7×10^4 s leads to a rapid grain coarsening accompanied by a sharp decrease in N . Then, the grain size distribution changes from a double peak to a single peak type, as shown in Figs.2(c) and 2(d). During this process, some coarse grains containing high density dislocations (Fig.5(a)) may be consumed by recovered growing grains in the surroundings. For annealing time above 7×10^4 s, the average grain size increases gradually accompanied with a little decrease in N , suggesting the occurrence of normal grain growth. Therefore, it is concluded from Figs.1–4 discussed above that a grain structure developed by continuous dynamic recrystallization (CDRX) operating during hot deformation only coarsens continuously during static annealing.

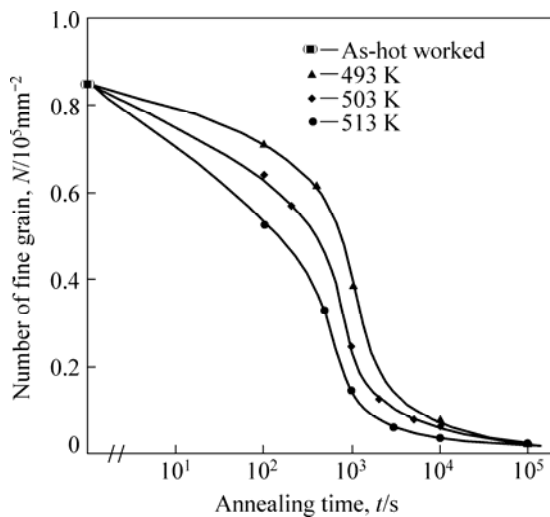


Fig.4 Effect of annealing temperature on relationship between number of fine grains with less than 10 μm in diameter per unit area, N , and annealing time

3.2 OIM microstructure

Typical OIM micrographs with the inverse pole figures for compression direction are shown in Fig.5. Figs.5(a), 5(b) and 5(c) correspond to the microstructures in Figs.1(a), 1(c) and 1(d), respectively. Disorientations (θ) $\theta > 2^\circ$, $\theta > 4^\circ$ are delineated by thin white and black lines, while high-angle boundaries including kink bands[11] with misorientations more than 15° are by bold black lines. Different grains correspond to different crystallographic orientations. It is clearly seen in Fig.5 that most of the grains developed have a strong texture near (0001) compared with those near (1010) or (1120). It is known[9] that extruded rod of Mg alloys has a strong texture in which the basal plane of the HCP lattice lies parallel to the extrusion direction (the compression direction in the present case). The basal plane rotates gradually from around 0° to near 90° to the compression axis with deformation. It is remarkable to note in Fig.5

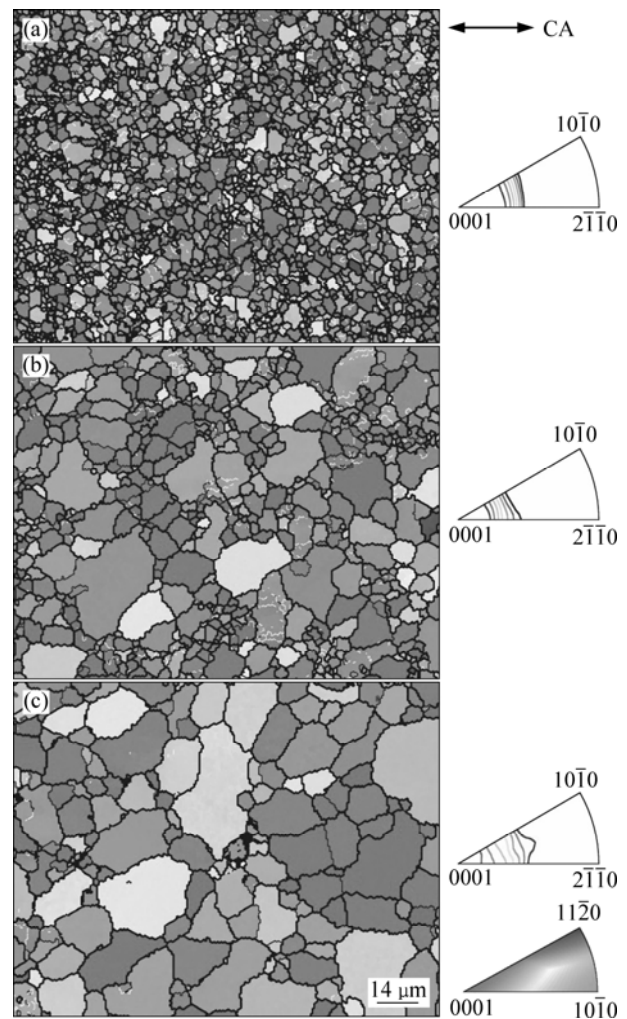


Fig.5 OIM micrographs and inverse pole figures of AZ31 alloy: (a) Deformed to $\varepsilon=1.2$ at 573 K and at $3 \times 10^{-1} \text{ s}^{-1}$, followed by isothermal annealing at 503 K for 10^3 s (b), and 10^4 s (c) (Thin white lines correspond to boundaries of misorientation $> 2^\circ$, thin black line $> 4^\circ$ and thick black lines $> 15^\circ$, respectively. Grains corresponding to crystallographic orientations indicate in inverse pole figure.)

that such a deformation texture with (0001) perpendicular to the compression axis exists stably even after full annealing with increasing time. It is concluded that strain-induced fine grains evolved in Mg alloys can grow remarkably and, in contrast, the deformation texture is scarcely changed with annealing.

It is suggested by Fig.5 that the texture of wrought Mg alloy may be hardly controlled by using conventional methods, i.e. plastic working followed by annealing. It is also seen in Fig.5(a) that dislocation boundaries with low angle misorientations are developed in remained coarse grains, and the cumulative misorientations near the original grain boundaries are within a few degrees, i.e. there is almost no lattice orientation gradient evolved [9]. This is in contrast with the cases of hot-deformed grains

and conventional DRXed grains in cubic metals. Namely, some high orientation and strain gradients always form near the grain boundaries, leading to nucleation with various orientations followed by long range grain boundary migration[13–16]. Thus, deformation process accompanied with various strain paths, such as multi-directional forging (MDF)[8], may be useful for texture modification of Mg alloy.

Fig.6 shows the changes in the distribution of misorientation angles with increasing annealing time. The distribution after annealing for 10^2 s is similar to that for an as-deformed matrix in Fig.6(a), and Fig.6(b) corresponds to stage 1 of annealing processes in Fig.3. Further annealing for a longer period, corresponding to stage 3, leads to a rapid drop of the fraction of LABS accompanied with a little increase in the average misorientation angle. This corresponds to stage 2 in Fig.3. In stage 3, the shape of the distribution curve as well as the average value of θ scarcely changes while grain coarsening gradually takes place (Fig.3).

3.3 Kinetics of recrystallization

The grain growth during recrystallization is generally thought to be the migration of grain boundaries or a thermally activated atom transport process. Thus, the

temperature dependence of the annealing time may be expected to exhibit Arrhenius behavior here expressed mathematically as

$$T=t_0\exp[-Q/(RT)] \tag{1}$$

where R is the gas constant, T is the absolute temperature, t_0 is the preexponential constant (annealing time at infinite temperature) and Q is the activation energy responsible for grain growth.

The annealing time obtained from the present experiment of AZ31 alloy is shown in Fig.7 plotted on a logarithmic scale versus the reciprocal of the absolute temperature on a linear scale. From the slope of the lines giving the value of $-Q/R$ the activation energy can be deduced to be (125 ± 10) kJ/mol (Fig.7) both for $D=7 \mu\text{m}$ and for $N=3 \times 10^4 \text{mm}^{-2}$ (When D and N in stage 2 are constant (Fig.3 and Fig.4)), indicating the accuracy of the data in this experiment. It is clearly seen that the value is very close to the self-diffusion activation energy of atoms in magnesium alloy (about 135 kJ/mol), and thus demonstrates that grain growth process is mainly controlled by the self diffusion of atoms. Although impurity atoms might accumulate in the grain boundaries and exert a retarding force on grain boundary migration, they do not change the grain growth activation energy[17].

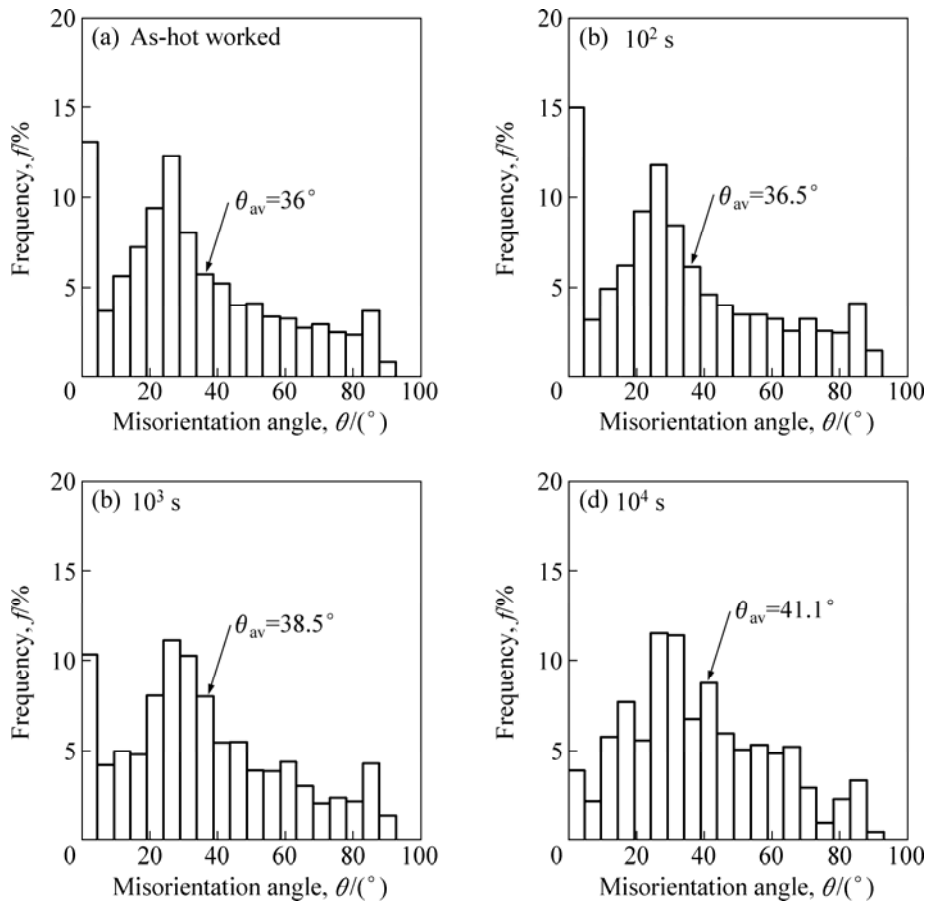


Fig.6 Distribution of misorientation angles with increasing annealing time

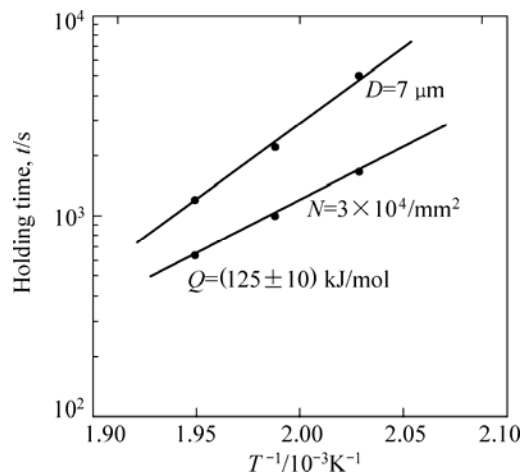


Fig.7 Plot of annealing time versus absolute temperature on linear scale according to Arrhenius equation

4 Conclusions

1) Annealing time dependence of the average grain size is categorized into three stages, i.e. an incubation period of grain growth from 0 to 7×10^2 s, rapid grain coarsening from 7×10^2 s to 7×10^4 s and normal grain growths above around 7×10^4 s, respectively. The number of fine grains per unit area, however, is reduced remarkably even in stage 1. It is concluded, therefore, that grain growth takes place continuously during the whole period of annealing.

2) The deformation texture with the basal plane (0001) perpendicular to the compression axis can exist stably with increasing annealing time and scarcely changes even after full annealing.

3) The annealing processes operating in hot-deformed Mg alloy with fine grains, developed by CDRX, are mainly controlled by grain growth without texture change, which is continuous static recrystallization (cSRX).

4) The activation energy Q responsible for grain growth can be deduced to be (125 ± 10) kJ/mol close to the self diffusion activation energy of atoms in magnesium alloy (135 kJ/mol), demonstrating a grain growth process mainly controlled by the self-diffusion of atoms.

References

[1] GALIYEV A, KAIBYSHEV R. Superplasticity in a magnesium alloy subjected to isothermal rolling [J]. *Scripta Materialia*, 2004, 51(2): 89–93.

- [2] BUSSIBA A, BEN ARTZY A, SHTECHMAN A, IFERGAN S, KUPIEC M. Grain refinement of AZ31 and ZK60 Mg alloys()—towards superplasticity studies [J]. *Materials Science and Engineering A*, 2001, 302(1): 56–62.
- [3] OHISHI K, MENDIS C L, HOMMAB T, KAMADO S, OHKUBO T, HONO K. Bimodally grained microstructure development during hot extrusion of Mg-2.4Zn-0.1Ag-0.1Ca-0.16Zr (at.%) alloy[J]. *Acta Materialia*, 2009, 57: 5593–5604.
- [4] PRASAD Y V P K, RAO K P. Effect of crystallographic texture on the kinetics of hot deformation of rolled Mg-3Al-1Zn alloy plate [J]. *Materials Science and Engineering A*, 2006, 432(1/2): 170–177.
- [5] YAMASHITA A, HORITA A, LANGDON T G. Improving the mechanical properties of magnesium and a magnesium alloy through severe plastic deformation [J]. *Materials Science and Engineering A*, 2001, 300(1/2): 142–147.
- [6] KIM W J, HONG S I, KIM Y S, MIN S H, JEONG H T, LEE J D. Texture development and its effect on mechanical properties of an AZ61 Mg alloy fabricated by equal channel angular pressing [J]. *Acta Materialia*, 2003, 51(11): 3293–3307.
- [7] HELLMIG R J, LAMARK T T, POPOV M V, JANEČEK M, ESTRIN Y, CHMELÍK F. Influence of equal-channel angular pressing on the acoustic emission behaviour of magnesium alloy AZ31 under compression [J]. *Materials Science and Engineering A*, 2007, 462(1/2): 111–115.
- [8] XING J, SOHDE H, YANG X, MIURA H, SAKAI T. Ultra-fine grain development in magnesium alloy AZ31 during multi-directional forging under decreasing temperature conditions [J]. *Mater Trans*, 2005, 46(20): 1646–1650.
- [9] YANG X, MIURA H, SAKAI T. Dynamic evolution of new grains in magnesium alloy AZ31 during hot deformation [J]. *Mater Trans*, 2003, 44(1): 197–203.
- [10] AL-SAMMAN A, GOTTSTEIN G. Dynamic recrystallization during high temperature deformation of magnesium [J]. *Materials Science and Engineering A*, 2008, 490(1/2): 411–420.
- [11] BEAUSIR B, SUWAS S, TÓTH L S, NEALE K W, FUNDENBERGER J J. Analysis of texture evolution in magnesium during equal channel angular extrusion [J]. *Acta Materialia*, 2008, 56(2): 200–214.
- [12] DEL VALLE J A, RUANO O A. Influence of texture on dynamic recrystallization and deformation mechanisms in rolled or ECAPed AZ31 magnesium alloy [J]. *Materials Science and Engineering A*, 2008, 487(1/2): 473–480.
- [13] HUMPHREYS F J, HATHERLY M. *Recrystallization and related annealing phenomena* [M]. Oxford, UK: Pergamon Press, 2004: 127–392.
- [14] SAKAI T, JONAS J J. Dynamic recrystallization: Mechanical and microstructural considerations [J]. *Acta Metallurgica*, 1984, 32(2): 189–209.
- [15] HANSEN N: *Evolution of deformation microstructure in 3D* [M]. Denmark: Riso National Lab., 2004.
- [16] WUSATOWSKA-SARNEK A M, MIURA H, SAKAI T. Influence of deformation temperature on microstructure evolution and static recrystallization of polycrystalline copper [J]. *Mater Trans*, 2001, 42 (11): 2452–2459.
- [17] LIU F, KIRCHHEIM R. Comparison between kinetic and thermodynamic effects on grain growth[J]. *Thin Solid Films*, 2004, 466(1/2): 108–113.

(Edited by LI Xiang-qun)